DESIGN AND EXPERIMENT OF AN INTEGRATED PRUNING, THRESHING AND BRANCH CHOPPING MACHINE FOR GREEN PRICKLY ASH
/
青花椒整枝脱粒碎枝一体机设计与试验

Hao WANG[1)]; Yanjun ZHOU*[1)]; Chuanyao LIN[1)]; Jian WU[1)]; Jia DENG[1)]; Xiaobo ZHOU[1)]
[1)] Sichuan Academy of Agricultural Machinery Science / China;
Tel: +86-15281031885; E-mail: 1550698497@qq.com
DOI: https://doi.org/10.35633/inmateh-76-98

Keywords: *Green prickly ash; Structural Design; Finite Element Analysis; Response Surface Experiment*

ABSTRACT
Aiming at the difficulty and low efficiency of threshing green prickly ash, a small-sized integrated pruning, threshing and branch chopping machine driven by a DC motor was designed and studied. The dynamic and static analyses of the tubular straight-cut threshing device and the clamping traction roller-cutting device were carried out respectively. The results show that the maximum shear stress on the green prickly ash branch during the cutting and separation process is 0.156 MPa. The maximum stress on the cutting blade of the clamping traction roller-cutting device is 333.99 MPa, and the maximum strain is 0.0017, which fully meets the usage requirements. The response surface analysis experiment was conducted with the moisture content of green prickly ash branches and the motor speed as the influencing factors and the undamaged threshing rate as the index. After optimization and solution, it was found that when the moisture content of green prickly ash branches was 43% and the motor speed was 1488 r/min, the undamaged threshing rate reached 95.9%, and the integrated pruning, threshing and branch chopping machine for green prickly ash reached the optimal working state.

摘要
针对青花椒脱粒困难，效率较低，设计研究了一款采用直流电机驱动的小型整枝脱粒碎枝一体机。分别对管状直切脱粒装置和夹持式牵引滚切装置进行显示动力学和静力学分析，其结果表明，在切割分离过程中花椒穗枝受到的最大剪切应力为 0.156MPa。夹持式牵引滚切装置的切割刀片所受的最大应力为 333.99MPa，最大应变为0.0017，完全满足使用要求。以花椒穗枝含水率和电机转速为影响因素，以花椒未损伤摘净率为指标进行响应面分析试验，优化求解后得到在花椒穗枝含水率为 43%，电机转速为 1488r/min 时，花椒未损伤摘净率达到 95.9%，青花椒整枝脱粒碎枝一体机达到最优工作状态。

INTRODUCTION
Green prickly ash, as a distinctive crop, is rich in nutritional and medicinal value. Due to its strong adaptability, high demand, good economic benefits and easy cultivation, the planting area and output of prickly ash in Sichuan Province have been expanding at an annual rate of about 30%. When harvesting green prickly ash, the branches bearing fruits are cut together with the fruits, which not only improves the harvesting efficiency but also promotes the growth of the prickly ash trees in the following year. The harvested branches are then subjected to threshing to complete the harvesting process *(Zhibo X. et al., 2022)*.

At present, the threshing of green prickly ash is mainly done manually, by beating the dried green prickly ash with bamboo sticks or wooden rods. This method is labor-intensive and inefficient and cannot meet the rapid development of the prickly ash industry. Therefore, it is necessary to design and develop more lightweight, easy-to-operate, reliable, high-threshing efficiency and low-damage rate prickly ash threshing equipment. *Yang L. et al.* designed a rotary shearing type green prickly ash harvesting device, which uses a reciprocating cutter to achieve the shearing function. They built a simulation model of the prickly ash branch shearing using ANSYS/LS-DYNA, determined the optimal tooth shape parameters, and verified through a three-factor quadratic regression orthogonal combination experimental that under the optimal working parameters, the average harvesting efficiency of green prickly ash per person per branch was 10.95kg/h, the average cleaning rate was 95.57%, and the average damage rate was 12.87% *(Yang L. et al., 2024)*.

Hao Wang, Assistant Engineer; Yanjun Zhou, Senior Engineer; Chuanyao Lin, Engineer;
Jian Wu, Engineer; Jia Deng, Senior Agronomist; Xiaobo Zhou, Senior Agronomist;

Jiang Q. et al. designed an automatic recognition prickly ash harvester, mainly including the visual recognition part, the mechanical arm movement part, the fruit storage part, and the vehicle drive part. Through dynamic simulation, the parts can be coordinated to achieve visual recognition and positioning harvesting of prickly ash fruits. Based on the existing structure, the picking device, transmission device and other components were designed and analyzed based on the principle of comb brushing. Using ADAMS software, the response surface simulation analysis experimental was conducted with the rotational speed of the comb brushing roller, the distance between the comb brushing roller and the feeding port, and the distance between the two comb brushing rollers as the influencing factors, and the undamaged cleaning rate of prickly ash fruits as the detection target. Under the optimal parameters, the undamaged cleaning rate of prickly ash fruits was 96.6% *(Jiang Q. et al., 2023)*.

This paper focuses on the design and development of a small-sized integrated machine for pruning, threshing and crushing branches for the green prickly ash harvesting process, with the aim of providing certain references and inspirations for the design of mechanical equipment in the green prickly ash harvesting process.

MATERIAL AND METHODS

Main Structural Components

The overall design of the machine is based on the "cutting at the base" of the green prickly ash. After converting the pepper tree into pepper branches, the branches are processed for fruit picking and branch crushing using a rotary tubular cutting technology *(Shao W., et al., 2023; Yexin L., et al., 2022)*. The pepper fruits are obtained, and the crushed branches are used as fertilizer and returned to the field. The overall structure is shown in Fig. 1, mainly consisting of a frame, a clamping traction roller cutting device, a reversing reducer, a transmission chain, a tubular straight-cutting and threshing device, a transmission belt, a motor, etc.

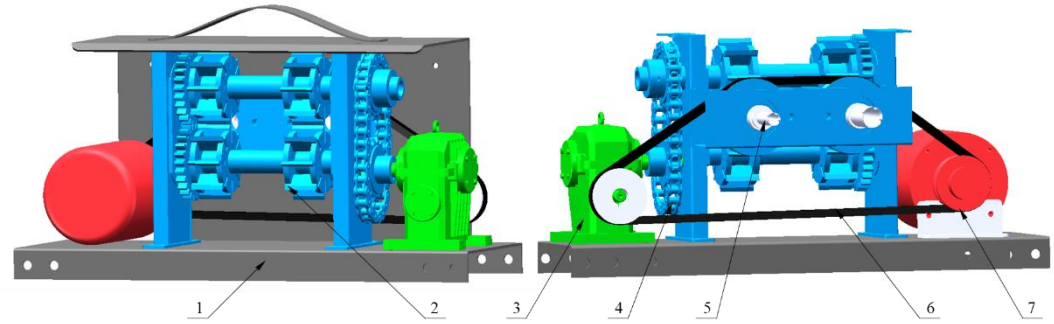

Fig. 1 - Structure Diagram of the Integrated Machine for Branch Pruning, Threshing and Branch Crushing of Green Prickly Ash

1-Frame; 2-Clamping Traction and Rolling Cutting Device; 3-Reversing Reducer; 4-Transmission Chain; 5-Tubular Straight Cutting and Threshing Device; 6-Transmission Belt; 7-Motor

Working Principle

An Integrated Pruning, Threshing and Branch Chopping Machine for Green Prickly Ash uses a DC motor as the power source, equipped with a battery, which is convenient for use in the field without AC power. It adopts belt drive, worm gear drive and gear drive mechanisms to drive the tubular straight-cutting destemming device and the clamping traction roller cutting device respectively. During operation, the pruned branches of green prickly ash are fixed by the clamping wheels and move in a fixed direction driven by the chain. When passing through the tubular cutting knife, the prickly ash fruits are cut off from the branches by the low-speed rotation and feeding process of the tubular knife, completing the picking of prickly ash. The branches are crushed after passing through the clamping knife *(Du P., et al., 2024; Li R., 2022)*. This picking device can achieve destemming and crushing of branches of different thicknesses by changing the diameter of the tubular knife. At the same time, it can feed multiple branches simultaneously to increase the picking efficiency.

Design of Key Components

Tubular Straight Cutting and Threshing Device

The threshing device uses a serrated tubular cutting knife. The circular ring with teeth and cutting edge type tool is fixed in the bearing sleeve on the bearing seat through a threaded connection and rotates at high speed driven by a DC high-speed motor via belt drive, separating the clusters and branches. During operation, the force analysis of the device is shown in Fig. 2.

In the figure, β is the cutting edge angle of the tool, θ is the friction angle of the tool, F_N is the pressure of the prickly ash clusters and branches on the wedge surface of the cutting edge during cutting, F_s is the pressure of the clusters and branches on the bottom surface of the cutting edge during cutting, F_1 is the resistance force on the cutting edge, F_2 is the cutting force required for cutting the prickly ash clusters and branches, f_1 is the friction force on the bottom surface of the cutting edge, and f_2 is the friction force on the wedge surface of the cutting edge. The required cutting force F_2 during operation is given by equation (1).

$$F_2 = F_1 + F_S \tan\theta + F_N(\tan\theta\cos\beta + \sin\beta) \quad (1)$$

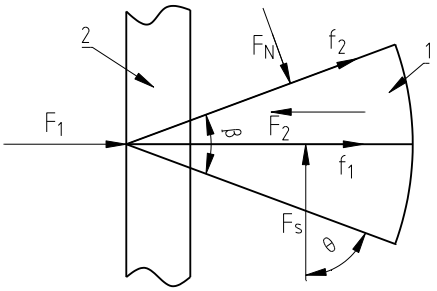

Fig. 2 - Force Analysis Diagram of Tubular Direct Cutting Threshing Device
1 - Cutting Tool; 2 - Pepper Spike Branch

Clamping Traction and Rolling Cutting Device

The structural diagram of the clamping traction rolling cutting device is shown in Fig. 3. It uses two rollers rotating in opposite directions. The surface of the rollers is processed with anti-slip teeth. The pepper branches are clamped between the rollers. The rollers rotate to pull the branches along, avoiding the branches from slipping due to rotation. The cutting device installs a fixed knife on the frame and a cutting knife on the rotating roller. During the rotation of the roller, the cutting knife and the fixed knife interact with each other to crush and cut the branches after the green prickly ash fruits are removed.

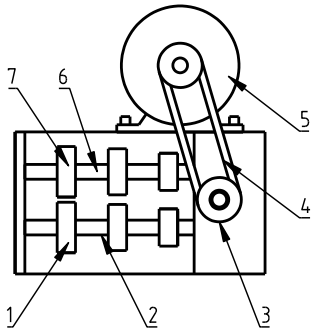

Fig. 3 - Structural schematic diagram of the clamping-type traction and cutting device
1-Lower clamping wheel; 2-Lower clamping wheel drive shaft; 3-Pulley; 4-Belt;
5-Drive motor;6-Upper clamping wheel drive shaft; 7-Upper clamping wheel

Main Technical Parameters

This design takes the rate of intact and undamaged pepper pods harvested and the rate of crushing of pepper branches as the main performance indicators of the entire machine. Based on the geometric and physical parameters as well as the growth and physiological characteristics of green prickly ash, the main technical parameters of the integrated machine for pruning, threshing and crushing of green prickly ash are shown in Table 1.

Table 1

Main Technical Parameters of the Integrated Machine for Pruning, Threshing and Crushing of Green Prickly Ash

Parameter Name	Parameter Value
Overall dimensions (L×W×H)/(mm)	480×250×650
Overall machine weight/(kg)	24
Motor power/(kW)	550
Gear ratio of reversing reducer	1:20
Rated rotational speed of cutting blade/(r/min)	2000
Rated rotational speed of clamping wheel/(r/min)	100
Feed speed of pepper branches/(mm/s)	400
Applicable diameter of pepper branches/(mm)	10~25
Applicable length of pepper branches/(mm)	150~2000

RESULTS

PERFORMANCE SIMULATION ANALYSIS OF TUBULAR STRAIGHT CUTTING THRESHING DEVICE

Simulation Model

A tubular straight cutting threshing device operation model was established using SolidWorks 2020, and it was simplified. The length direction of the pepper branches was regarded as a standard cylinder, and the bending and taper changes of the branches were ignored. The influence of the sharp spines and the surface of the branches was also ignored, as well as the influence of the pepper fruits and branches and leaves. A branch and spike separation model was established *(Li Y., 2023; Shan H., et al., 2022)*. According to the geometric and physical parameters of pepper, the diameter of the pepper branch was set to 12 mm, the diameter of the pepper spike branch was set to 4 mm, and the diameter of the circular cutting knife holes was set to 22 mm.

The model was established using SolidWorks 2020. The model was imported into the Workbench 19.2 LS-DYNA module. The material properties of the pepper branches are shown in Table 2. The material of the circular cutting knife was selected as structural steel. The model was divided into grids, with tetrahedral elements as the basic type. The size was set at 2 mm. After the division, there were 6066 nodes and 22,250 elements. The simulation conditions are shown in Table 3.

Table 2

Properties of Cinnamon Branch Materials

Parameter Name / Measure unit	**Value**
Density / (kg/m^3)	850
Young's Modulus X direction / (MPa)	115
Young's Modulus Y direction / (MPa)	17.25
Young's Modulus Z direction / (MPa)	8.63
Poisson's Ratio XY / (r/min)	0.38
Poisson's Ratio YZ / (r/min)	0.038
Poisson's Ratio XZ / (mm/s)	0.038
Shear Modulus XY / (MPa)	41.67
Shear Modulus YZ / (MPa)	4.16
Shear Modulus XZ / (MPa)	8.31
Maximum Equivalent Plastic Strain EPS	0.1

Table 3

Simulation Initial Conditions Table

Parameter Name	**Value**
Type	Frictional
Friction Coefficient	0.4
Dynamic Coefficient	0.3
Erosion algorithm	Single Surface
Velocity / (mm/s)	400
Rigid Body Rotation / (r/min)	2000
End Time / (s)	0.5

Simulation Results and Analysis

The shear stress exerted on the pepper sprout branches during the cutting and separation process is shown in Fig. 4. When the circular cutter initially starts to cut the pepper sprout branches, the shear stress on the sprout branches is 0. As the circular cutter cuts into the pepper sprout branches, the high-speed rotation of the circular cutter generates a significant shear force on the sprout branches, causing the shear stress to rapidly increase and reach a peak of 0.156 MPa at 0.05 s. At this point, the sprout branches undergo deformation. After the axial coarse fibers of the pepper sprout stem are cut off, the shear stress drops sharply and finally approaches a horizontal line. The contact moment of the circular cutter during the cutting and separation process is shown in Fig. 5.

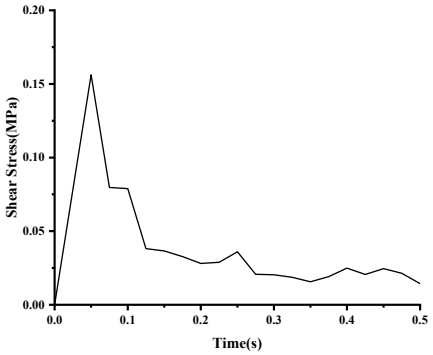

Fig. 4 - Shear Stress Change Curve

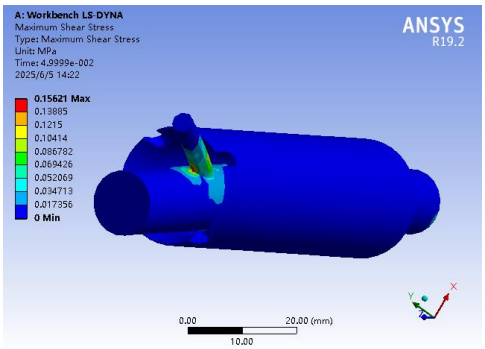

Fig. 5 - Cutting Contact Instantaneous Diagram

PERFORMANCE SIMULATION ANALYSIS OF THE CLAMPING TRACTION ROLLING CUTTING DEVICE

The clamping traction rolling cutting device, as one of the core components of the entire machine, experiences varying degrees of bending deformation on the blades on the clamping conveyor wheels during actual operation. Therefore, it is the most prone part to failure in the entire machine. To verify whether it meets the design requirements, a static analysis was conducted using the ANSYS Workbench simulation software.

Model Establishment

The clamping traction rolling cutting device operation model was established using SolidWorks 2020, and the material was selected as 45 steel. The model was imported into the software and meshed. The basic type of the mesh was tetrahedral elements, with a size of 1 mm. After meshing, there were 287638 nodes and 59612 elements. There were a total of 8 blades on the clamping traction rolling cutting device, but only one blade was in operation during the cutting process. Therefore, only one blade was subjected to load for static analysis. Based on the displayed dynamic model simulation results, boundary conditions were set to ensure the stability and reliability of the device. A driving torque of 100 N·mm was applied to the clamping conveyor wheel, and a vertical force of 2000 N was applied to the blade of the clamping conveyor wheel.

Simulation Results

A finite element analysis was conducted on the clamping traction rolling cutting device. The total displacement analysis cloud map is shown in Fig. 6. From the figure, it can be seen that the displacement variation at any point in the middle of the cutting blade is very small, and the maximum displacement occurs at the middle, but it is only 0.0033 mm. The stress analysis cloud map is shown in Fig. 7, and the maximum stress on the part is 333.99 MPa, which is at the thinnest part of the cutting blade. The strain analysis cloud map is shown in Fig. 8, and the maximum strain is 0.0017, which is also concentrated at the thinnest part of the cutting blade. Based on the yield strength of 45 steel ≥ 355 MPa and the tensile strength of 600 MPa, it can be known that the designed part can fully meet the usage requirements.

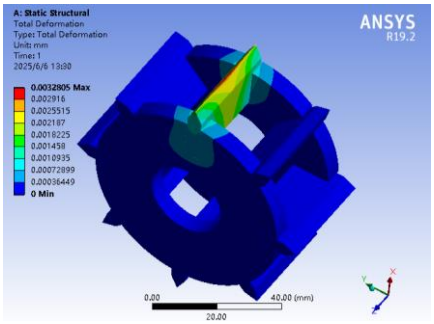

Fig. 6 - Total Displacement Analysis Cloud Image

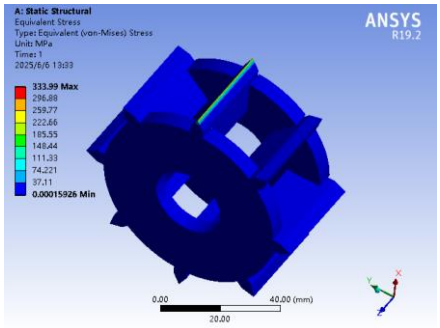

Fig. 7 - Stress Analysis Nephogram

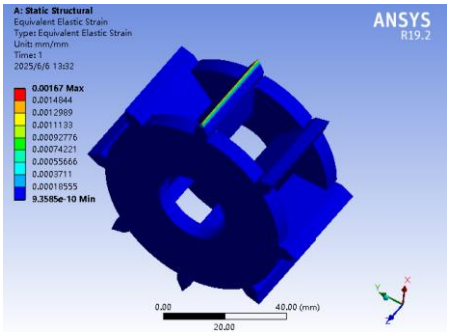

Fig. 8 - Strain Analysis Cloud Image

EXPERIMENTAL VERIFICATION

Experimental Indicators and Measurement Methods

In this experiment, the moisture content of the pepper branches and the motor speed were taken as the influencing factors, and the undamaged and clean yield of the pepper was used as the evaluation indicator *(Zhang Y., 2024; Shao W., et al., 2020)*. The calculation formula for the evaluation indicators is shown in equation (2).

$$Y = \frac{n_1 - n_2}{n} \times 100\% \quad (2)$$

where:

Y - Unharmed yield rate, [%];

n_1 - Separated quantity, [pieces];

n_2 - Damaged quantity, [pieces];

n - Total quantity, [pieces];

The response surface simulation analysis experiment was designed using the Design-Expert12 software. All the experimental factors were represented by the three levels of coding -1(low), 0(medium), and +1(high). The factor coding table is shown in Table 4.

Table 4

Coding Table of Experimental Factors

Code	Factor	
	Water content of pepper fruit branches X_1/(%)	**Motor speed X_2/(*r/min*)**
-1.414	25.8579	1075.74
-1	30	1200
0	40	1500
1	50	1800
1.414	54.1421	1924.26

Experimental Results and Analysis

Experimental Results

The Experimental plan and results are shown in Table 5.

Table 5

Experimental Plan and Results

Experimental Number	Water content of pepper fruit branches X_1/(%)	Motor speed X_2/(*r/min*)	Unharmed yield rate Y/(%)
1	25.8579	1500	95.9
2	30	1800	94.9
3	30	1200	94.6
4	40	1500	96.2
5	40	1500	96.6
6	40	1075.74	94.5
7	40	1500	95.7
8	40	1500	96.7
9	40	1500	96.5
10	40	1924.26	93.8
11	50	1200	94.1
12	50	1800	93.9
13	54.1421	1500	94.3

According to the data in Table 3, using the Design-Exper12 software, a variance regression analysis was conducted on the undamaged and stripped yield rate of pepper, and the regression equation model reflecting the relationship of its change with the experimental factors was obtained, as shown in equation (3).

$$Y = 96.34 - 0.4703X_1 - 0.1112X_2 - 0.1250X_1X_2 - 0.6825X_1^2 - 1.16X_2^2 \quad (3)$$

Analysis of Variance

Based on the experimental data, an analysis of variance was conducted and the results after removing the insignificant items are shown in Table 6.

Table 6

Analysis of Variance Table for the Uninjured and Cleaned Rate of Pepper

Source	Sum of Squares	df	Mean Square	F-value	P-value
Model	13.25	5	2.65	18.58	0.0006
X_1	1.77	1	1.77	12.41	0.0097
X_2	0.0990	1	0.0990	0.6942	0.4322
X_1X_2	0.0625	1	0.0625	0.4383	0.5291
X_1^2	3.24	1	3.24	22.72	0.0020
X_2^2	9.32	1	9.32	65.36	< 0.0001
Residual	0.9982	7	0.1426		
Lack of Fit	0.3462	3	0.1154	0.7080	0.5956
Pure Error	0.6520	4	0.1630		
R^2	0.9299				
Cor Total	14.25	12			

From the variance analysis of the undamaged and cleaned rate of the pepper in Table 4, it can be seen that the order of the magnitude of the influence of the interaction effects among the various factors on the impurity rate is X_2^2, X_1^2, X_1, X_2, X_1X_2. X_2^2, X_1^2, X_1, X_2 (the influence is extremely significant, $P<0.01$), and X_1X_2 has a relatively significant influence($0.05 \leq P<0.1$). The residual sum of squares $P=0.5956$ is not significant ($P>0.1$), which proves that there are no other main factors that affect the experimental indicators.

Response Surface Analysis

The moisture content of the pepper branches X_1, the motor speed X_2, and their interaction have significant effects on the undamaged and cleaned rate of the pepper. The response surface of the interaction between the moisture content of the pepper branches and the motor speed obtained using the Design-Exper12 software is shown in Fig. 9.

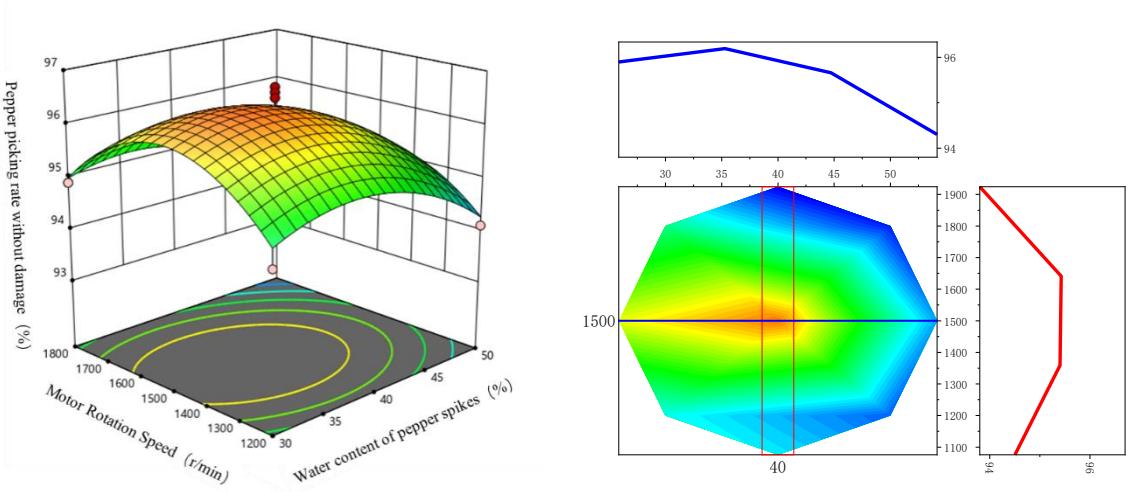

Fig. 9 - Influence of Factor Interaction on Impurity Content

The interaction effect of the moisture content of the pepper branches and the motor speed has a significant impact on the unharmed threshing rate of the pepper *(Li C., et al., 2024; Guo J., et al., 2023)*. When both factors are at their lowest levels, the unharmed threshing rate of the pepper reaches its minimum within the depicted range; when the moisture content of the pepper branches is at its lowest level, the unharmed threshing rate of the pepper is within a higher range; when the moisture content of the pepper branches is at its highest level, the unharmed threshing rate of the pepper is within a lower range. Under the same moisture content of the pepper branches, as the motor speed increases, the unharmed threshing rate of the pepper shows a trend of first increasing and then decreasing; under the same motor speed factor, as the moisture content of the pepper branches increases, the unharmed threshing rate of the pepper still shows a trend of first increasing and then decreasing.

Parameter Optimization and Verification Experiments

To achieve the optimal operating state of the integrated pruning, threshing, and branch-chopping machine for green prickly ash and to maintain a high undamaged threshing rate, the optimization module in Design-Expert 12 software was used to optimize and solve the regression model *(Huang Y., et al., 2024; Sun H., 2022)*.

To verify the above experimental conclusions, multiple verification experiments were conducted under the optimal working conditions, and the results are shown in Table 7. The experimental error is small and within the acceptable range, indicating that the regression equation is in good agreement with the actual situation and the model is reliable.

Table 6

Prediction and Verification Results Table

Parameters	Water content of pepper fruit branches X_1 / (%)	Motor speed X_2 / (r/min)	Unharmed yield rate Y / (%)
Predicted value	43	1488	96.1413
Verification value			95.9

CONCLUSIONS

Due to the difficulty and low efficiency in threshing of green prickly ash, a small-sized integrated machine for pruning, threshing and crushing of pepper branches was designed. It is driven by a DC motor. The pipe-shaped straight-cut threshing device and the clamping traction and rolling cutting device cooperate with each other to cut off the pepper fruit clusters, completing the pepper picking process while crushing the branches.

Finite element analyses were conducted on the pipe-shaped straight-cut threshing device and the clamping traction and rolling cutting device. The results showed that the maximum shear stress on the pepper clusters during the cutting and separation process was 0.156 MPa. The maximum displacement changes on the cutting blades of the clamping traction and rolling cutting device was only 0.0033 mm, and the maximum stress was 333.99 MPa, with a maximum strain of 0.0017, all concentrated at the thinnest part of the blade. Based on the material structure properties, the entire machine can fully meet the usage requirements.

Taking the moisture content of pepper clusters and the motor speed as influencing factors and using the undamaged and fully picked pepper rate as the index, a response surface simulation analysis experiment was designed. The regression equation model of the relationship with the changes of the experimental factors was obtained and optimized. When the moisture content of the pepper clusters was 43% and the motor speed was 1488 r/min, the undamaged and fully picked rate of the pepper reached 95.9%, which was the optimal working state of the designed integrated machine for pruning, threshing and crushing of green prickly ash branches.

REFERENCES

[1] Du P., Chen S., Li X., (2024). Green Prickly Ash Fruits Counting Based on Improved Deep Sort and Optimized Yolov5s. *Frontiers in Plant Science*, Vol. 15, pp. 151417682-1417682, DOI: 10.3389/FPLS.2024.1417682

[2] Guo J., Xiao X., Miao J. (2023). Design and Experiment of a Visual Detection System for Zanthoxylum-Harvesting Robot Based on Improved YOLOv5 Model. *Agriculture*, Vol. 13, Issue 4, pp, DOI: 10.3390/AGRICULTURE13040821

[3] Huang Y., Zhong Y., Zhong D., (2024). Pepper-YOLO: a lightweight model for green pepper detection and picking point localization in complex environments. *Frontiers in Plant Science*, Vol. 15, pp. 3151508258-1508258, DOI: 10.3389/FPLS.2024.1508258

[4] Jiang Q., Wan Z., Wang W. (2023). Design of Zanthoxylum Bungeanum Picker (花椒采摘机设计). *Agricultural Machinery Using & Maintenance*, Vol. 12, pp. 1-3+9, DOI: 10.14031/j.cnki.njwx.2023.12.001

[5] Li C., Shang S., Wang D., (2024). Peppercorn Harvester Design and Experiment (花椒采收机设计与试验). *Journal of Agricultural Mechanization Research*, Vol. 46, pp. 145-152, DOI: 10.13427/j.cnki.njyi.2024.10.013

[6] Li R., (2022). *Structure design and experiment of green Sichuan pepper picker based on branch trimming off (基于下桩的青花椒采摘机结构设计与试验).* (Degree Dissertation). Southwest University, Chongqing/China, DOI: 10.27684/d.cnki.gxndx.2022.001562

[7] Li Y. (2023). *Research on the cutting mechanism of green prickly ash branches and cutting device based on mechanical numerical model (基于力学数值模型的青花椒枝条切割机理和切枝装置研究). (*Degree Dissertation). Southwest University, Chongqing/China, DOI: 10.27684/d.cnki.gxndx.2023.003277

[8] Shan H., Bin L., Yuanzhe A. (2022). Comprehensive study on nutritional, flavour and metabolite characteristics of green prickly ash (*Zanthoxylum schinifolium*) at different picking stages. *International Journal of Food Science & Technology*, Vol. 57, pp. 7961-7973, DOI: 10.1111/IJFS.16154

[9] Shao W., Wu Y., (2020). Design and Experiment of Device for Ring-cut Cluster Branch Separation Unit of Green Prickly ash Picking Machine (青花椒采收机环切式穗枝分离装置设计与试验). *Agricultural Engineering*, Vol. 10, pp. 78-83;

[10] Shao W., Wu Y., Zhang L., (2023). Design and Experiment of Automatic Feeding Device for Harvester of *Zanthoxylum schinifolium* (青花椒采收机自动喂入装置设计与试验). *Agricultural Technology & Equipment*, Vol. 10, pp. 57-59

[11] Sun H., (2022). *Optimal design and research of a comb-tooth-air-suction pepper harvester* (梳齿-气吸式花椒采收机优化设计与研究). (Degree Dissertation). Gansu Agricultural University, Gansu/China, DOI: 10.27025/d.cnki.ggsnu.2022.000109

[12] Yang L., Zhang Y., He Z. (2024). Design and experiment of the rotating shear picking device for green Sichuan peppers (旋转剪切式青花椒采摘装置设计与试验). *Transactions of the Chinese Society of Agricultural Engineering*, Vol. 40, pp. 72-83, DOI: 10.11975/j.issn.1002-6819.202310135

[13] Yexin L., Binjie L., Yiyao J. (2022). Study on the Dynamic Cutting Mechanism of Green Prickly Ash (*Zanthoxylum armatum*) Branches under Optimal Tool Parameters. *Agriculture*, Vol. 12, pp. 1165-1165, DOI: 10.3390/Agriculture 12081165

[14] Zhang Y. (2024). *Design and experiment of a rotating shear picking device for green Sichuan pepper based on down-pile* (基于下桩的旋转剪切式青花椒采摘装置设计与试验). (Degree Dissertation). Southwest University, Chongqing/China, DOI: 10.27684/d.cnki.gxndx.2024.002746

[15] Zhibo X., Xiaopeng H., Yuan H. (2022). A Real-Time Zanthoxylum Target Detection Method for an Intelligent Picking Robot under a Complex Background, Based on an Improved YOLOv5s Architecture. *Sensors*, Vol. 22, pp. 682-682, DOI: 10.3390/S22020682